A time- and wavelength-division multiplexing sensor network with ultra-weak fiber Bragg gratings

Zhihui Luo,[1, 2] Hongqiao Wen,[1,3,*] Huiyong Guo,[1,3] and Minghong Yang[1,3]

[1] *National Engineering Laboratory for Fiber Optic Sensing Technology, Wuhan University of Technology(WHUT), 122 Luo Shi Road, Hong Shan District, Wuhan, 430070, China*
[2] *China Three Gorges University, 8 University Avenue, Yichang, 443002, China*
[3] *Key Laboratory of Fiber optic sensing technology and information processing, Institute of Information, Wuhan University of Technology, 430070, China*
[*] *whq@whut.edu.cn*

Abstract: A time- and wavelength-division multiplexing sensor network based on ultra-weak fiber Bragg gratings (FBGs) was proposed. The low insertion loss and the high multiplexing capability of the proposed sensor network were investigated through both theoretical analysis and experimental study. The demodulation system, which consists of two semiconductor optical amplifiers and one high-speed charge-coupled device module, was constructed to interrogate 2000 serial ultra-weak FBGs with peak reflectivity ranging from −47 dB to −51 dB and a spatial resolution of 2 m along an optical fiber. The distinct advantages of the proposed sensor network make it an excellent candidate for the large-scale sensing network.

OCIS codes: (050.2770) Gratings; (060.3738) Fiber Bragg gratings, photosensitivity; (060.4230) Multiplexing; (060.4250) Networks.

References and links

1. W. Jin, "Multiplexed FBG sensors and their applications," Proc. SPIE **3897**, 468–479 (1999).
2. C. S. Kim, T. H. Lee, Y. S. Yu, Y. G. Han, S. B. Lee, and M. Y. Jeong, "Multi-point interrogation of FBG sensors using cascaded flexible wavelength-division Sagnac loop filters," Opt. Express **14**(19), 8546–8551 (2006).
3. J. Ou and Z. Zhou, "Optic fiber Bragg-grating-based sensing technologies and their applications in structural health monitoring," Proc. SPIE **6595**, 01–08 (2007).
4. G. Gagliardi, M. Salza, P. Ferraro, and P. De Natale, "Fiber Bragg-grating strain sensor interrogation using laser radio-frequency modulation," Opt. Express **13**(7), 2377–2384 (2005).
5. W. H. Chung and H. Y. Tam, "Time- and wavelength-division multiplexing of FBG sensors using a semi-conductor optical amplifier in ring cavity configuration," IEEE Photon. Technol. Lett. **17**(12), 2709–2711 (2005).
6. M. Y. Jeon, J. Zhang, Q. Wang, and Z. Chen, "High-speed and wide bandwidth Fourier domain mode-locked wavelength swept laser with multiple SOAs," Opt. Express **16**(4), 2547–2554 (2008).
7. G. D. Lloyd, L. Bennion, L. A. Everall, and K. Sugden, "Novel resonant cavity TDM demodulation scheme for FBG sensing," in *Proceedings of Lasers and Electro-Optics*, San Francisco, CA, **CWD4**(2004).
8. Y. B. Dai, Y. J. Liu, J. S. Leng, G. Deng, and A. Asundi, "A novel time- division multiplexing fiber Bragg grating sensor interrogator for structural health monitoring," Opt. Lasers Eng. **47**(10), 1028–1033 (2009).
9. C. C. Chan, W. Jin, D. J. Wang, and M. S. Demokan, "Intrinsic crosstalk analysis of a serial TDM FBG sensor array by using a tunable laser," Proc. LEOS **36**, 2–4(2000).
10. Y. M. Wang, J. M. Gong, D. Y. Wang, B. Dong, W. Bi, and A. Wang, "A quasi-distributed sensing network with time-division-multiplexed fiber Bragg gratings," IEEE Photon. Technol. Lett. **23**(2), 70–72 (2011).
11. Y. M. Wang, J. M. Gong, D. Y. Wang, T. J. Shilig, and A. Wang, "A large Serial time-division multiplexed fiber Bragg grating sensor network," J. Lightwave Technol. **30**(17), 2751–2756 (2012).
12. H. Y. Guo, J. G. Tang, X. F. Li, Y. Zheng, and H. F. Yu, "On-line writing weak fiber Bragg gratings array," Chin. Opt. Lett. **11**(3), 030602–030605 (2013).
13. A. V. Xabier, M. L. Sonia, C. Pedro, and G. H. Miguel, "100 km BOTDA temperature sensor with sub-meter resolution," Proc. SPIE **8421**, 842117, 842117-4 (2012).
14. M. L. Zhang, Q. Z. Sun, Z. Wang, X. Li, H. Liu, and D. Liu, "A Large Capacity Sensing Network with Identical Weak Fiber Bragg Gratings Multiplexing," Opt. Commun. **285**(13-14), 3082–3087 (2012).
15. Z. Wang, Q. Z. Sun, and M. L. Zhang, "A Distributed Sensing System Based on Low-Reflective-Index Bragg Gratings," in *Proceedings of Photonics and Optoelectronics (SOPO)*, Wuhan, **1-3**(2011).

#194091 - $15.00 USD Received 17 Jul 2013; revised 12 Sep 2013; accepted 16 Sep 2013; published 20 Sep 2013

1. Introduction

Large-scale fiber Bragg grating (FBG) sensor networks have attractive prospects for major engineer monitoring because of their low cost and high multiplexing capability [1, 2]. Wavelength-division multiplexing (WDM) and time-division multiplexing (TDM) are two major multiplexing techniques for the expansion of the sensor network capacity [3, 4]. For the WDM method, the maximum number of FBGs is restricted by the ratio of the source spectral width over the dynamic wavelength range of an individual FBG sensor (i.e., typically a few nanometers). The TDM method utilizes different time delays between reflected pulses to distinguish sensors even with an identical wavelength and to relieve the spectral bandwidth issue. Several types of TDM networks with resonant cavity based on a semiconductor optical amplifier (SOA) have been proposed [5–8]. Limited by the gain of a single SOA, the interrogated FBGs with reflectivity of more than 1% are required. However, the multiplexing capacity is seriously limited by signal crosstalk among these normal FBGs [9]. A newly proposed optical time-domain reflectometry–fiber Bragg grating (OTDR–FBG) network with ultra-weak FBG array has been reported [10, 11]. This design employs a tunable laser (T-LD) as light source and distinguishes different FBGs via high-speed data acquisition. With the high-power tunable laser, the system has powerful detection of ultra-weak FBGs. However, due to slow speed of T-LD wavelength scanning and mass redundant data from no grating zones, the system could be inferred to subject a low speed for the precise interrogation.

Recently, our team has realized on-line writing of ultra-weak FBG arrays during drawing of ordinary single mode fibers (SMF) [12]. This array has no fusion loss and therefore shows high mechanical stability, which opens new possibility for further application of large-scale FBG networks. The main challenge of the large-scale sensor network is to massively multiplex FBG sensors and to quickly interrogate each FBG in the array. According to the latest report [11], the maximum multiplexing number of FBGs in an array is about 1000 in a single fiber, and the interrogation time for all sensors is more than a minute. In this paper, we reported a large-scale sensor network with time- and wavelength-division multiplexed (TDM + WDM) ultra-weak FBGs. The demodulation system consists of two SOAs and one high-speed charge-coupled device (CCD) module. The former is used to separate the reflected signals from different FBGs in the time domain, and the latter is utilized to detect the wavelength shift quickly. Compared to previous large-scale TDM schemes, the proposed system addresses FBGs directly and is expected to achieve rapid interrogation by synchronizing high-speed CCD modules with the SOAs. Moreover, using the TDM + WDM method, the multiplexing number of FBGs in a fiber is increased. The high multiplexing capability and the fast interrogation make the development of sensor networks containing thousands of FBGs possible.

2. Operation principle

Figure 1 illustrates the TDM + WDM ultra-weak FBG sensor network. A 2-6 nm light source consists of an amplified spontaneous emission source and a band-pass filter. The light is modulated and amplified into nanosecond pulses by the first SOA (SOA1, INPHENIX IPSAD1502). The pulses pass through the circulator and are launched into the serial TDM + WDM-FBG array (G_{11}, …, G_{1n}, …, G_{m1},…, G_{mn}), where G are FBGs; m is the number of sub-arrays in the entire array, each sub-array includes n FBGs with an identical wavelength, and all sub-arrays are different at the center wavelength. The total number of FBGs is $m \times n$ in such a large-scale array. Each FBG reflects part of the incident pulses back to the second SOA (SOA2, INPHENIX IPSAD1502) at different times. When the SOA2 is "on," the pulses arriving at the SOA2 are amplified. The pulses that pass through SOA2 are detected and then demodulated by a high-speed CCD module (IBSEN I-MON 80D) to obtain their wavelength shift and intensity directly. Both SOAs are driven by two trains of homogeneous pulses from a two-channel generator programmed to adjust the time delay between pulse trains. The SOA extinction ratio of above 40 dB can improve the optical signal-to-noise ratio (OSNR) [13]. Furthermore, the two SOAs have gain of more than 20 dB, which can increase the signal

#194091 - $15.00 USD Received 17 Jul 2013; revised 12 Sep 2013; accepted 16 Sep 2013; published 20 Sep 2013

power. The Erbium-doped fiber amplifier (EDFA) is used to amplify further the pulses. The data from the CCD detector are processed by an embedded computer and then are uploaded to a remote PC, which also controls the CCD module and the generator synchronously.

Given the different spatial positions of FBGs along the fiber, each FBG can be addressed separately by changing the time delay. The relation between the time delay (τ_i, $1 \le i \le n*m$) and the distance (L_i) of FBG_i from SOA is

$$\tau_i = \frac{2n_e L_i}{c} \tag{1}$$

$$(\tau_r + \tau_f) \le w \le \frac{2n_e d}{c}, \tag{2}$$

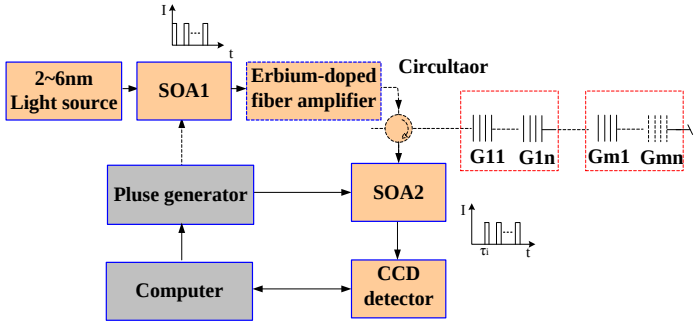

Fig. 1. Sensor network with an ultra-weak TDM + WDM-FBG array.

where n_e is the effective refractive index of the fiber; c is the speed of light in vacuum; w is the pulse width; d is the separation distance between FBGs; τ_r and τ_f are the rise-time and the fall-time of the modulated pulse, respectively. To eliminate signal overlapping, the time delay between two adjacent sensors should be more than the pulse width. During the initialization of the sensor network, the generator scans the time delay at a step of 1 ns, which corresponds to a resolution of 0.1 meter along the fiber. The CCD module detects the reflected signal and judges whether the reflected pulses are from FBGs according to the signal intensity. The CCD module then records the time delay at the peak power of the reflected signals from each FBG. When the sensor network runs, the generator reads these recorded delays and adjusts the time delay between pulse trains one by one. All FBGs are addressed in turn. The CCD module demodulates the reflected signal from every FBG and uploads the peak wavelength. The remote PC calculates the variation of the Bragg wavelength and infers the value of the monitored measurand. On the basis of the recorded time delay, the spatial position of each FBG can be calculated by using Eq. (1).

3. Experimental results and discussion

3.1 Optical Power Budget

The reflectivity of the ultra-weak FBG is generally less than –30 dB, and its reflected signals is weak, which may cause the sensor network to work improperly or as expected. Therefore, the optical power budget for the entire sensor network is introduced. The average light power refers to the radiation energy of all wavelengths in a second. Considering the narrow bandwidth of the reflected signal from the FBG (typically less than 0.2 nm), the average power of the reflected signal is far less than the broadband noise power of the SOA. When measuring the average power, the sensing signal will be submersed by the noise. The power spectral density (PSD) describes the distribution of signal energy in the wavelength axis and expresses the relative power of the sensing wavelength directly without the effect of other wavelengths. Therefore, the PSD is proposed to analyze the sensor network. Given that P_0 is

#194091 - $15.00 USD Received 17 Jul 2013; revised 12 Sep 2013; accepted 16 Sep 2013; published 20 Sep 2013

the PSD of the sensing wavelength from the source, the PSD of the modulated pulses P_m is expressed as

$$P_m = P_0 + 10\log(w/T) = P_0 + 10\log fw \tag{3}$$

where P_0 = −25 dBm; f is the modulation frequency (f = 40 KHz), and w is the pulse width (w = 16 ns). According to Eq. (3), the PSD of the modulated pulses will be 32 dB lower than the source. Figure 2 shows the PSD of the signals before and after modulation. A 28 dB decline is observed by using an optical spectra analyzer (OSA, YOKOGAWA AQ6370), which includes a 4 dB gain from SOA1. Therefore, the tested result is in good agreement with the theoretical calculation. The detection circuit of the OSA has integral effect and can continuously accumulate the signals in the response period. Thus, the PSD of the sensing signals is given as

$$P_{OSA} \geq P_m + A_{SOA1} + A_{EDFA} - P_c + P_{FBG} + A_{SOA2} - P_{other}, \tag{4}$$

where A_{SOA1} and A_{SOA2} are the gain of SOA1 and SOA2, respectively (A_{SOA1} = 4 dB; A_{SOA2} = 17 dB); A_{EDFA} is the gain of EDFA (A_{EDFA} = 28 dB); P_c is the insertion loss of the circulator (P_n = 2 dB); P_{FBG} is the peak reflectivity of the ultra-weak FBG; P_{other} includes the loss of connectors (P_{other} = 1 dB), and P_{OSA} is the sensitivity of the OSA. When the modulated pulses with 40 kHz launch into the sensor network and the peak reflectivity of the FBGs range from −47 dB to −51 dB, the measured PSD of the reflected pulses is from −59 dBm to −64 dBm, which is close to the theoretical calculation of −58 dBm to −62 dBm. The consistent result confirms the feasibility of the proposed optical power budget.

The CCD module works similar to the OSA. Given that the sensitivity of the proposed CCD module is −60 dBm, the detectable minimum power within the response time of 20 ms can be down to −107 dBm. Therefore, the minimum reflectivity of the FBG is −96 dB as power budget analysis. However, limited by the spontaneous noise of about −70 dBm from the SOA2, the reflectivity of the FBG should be more than −59 dB. Moreover, the dynamic range of the CCD detector is about 40 dB, and the response time can be adjusted from 20 ms to 1 s to improve further the dynamic range. Therefore, the theoretical dynamic range can reach up to 87 dB.

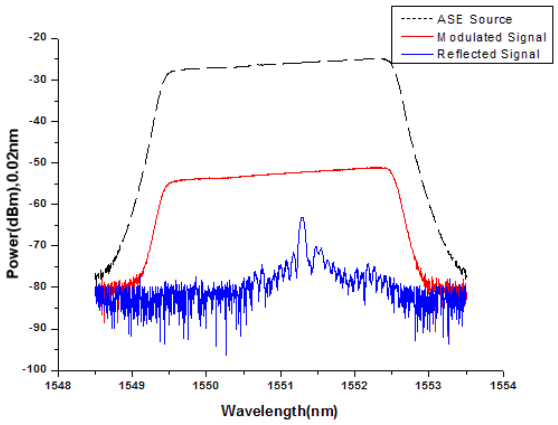

Fig. 2. PSD of the light source, modulated signal, and reflected signal.

3.2 Crosstalk and Multiplexing Capability

The multiplexing capacity of large-scale TDM sensor networks is mainly limited by two crosstalks, i.e., multiple-reflection crosstalk and spectral shadowing [9]. Multiple-reflection crosstalk describes the spectral distortion caused by the false signal, which undergoes

#194091 - $15.00 USD Received 17 Jul 2013; revised 12 Sep 2013; accepted 16 Sep 2013; published 20 Sep 2013

multiple reflections among the upstream FBGs and arrives at the detector at the same time with the real signal of the downstream FBGs. Related reports show that multiple-reflection crosstalk can be ignored when the reflectivity of FBG is less than 1% [8, 10]. Spectral shadowing refers to the spectral distortion of the downstream FBGs induced by the insertion loss of the upstream FBGs. For ultra-weak FBG array, the returned power from the *i*th (i = 1, 2 …, N) FBG at wavelength λ can be approximated as [11]

$$I_{ri}(\lambda) = I_0(\lambda)R(\lambda)(1-R(\lambda))^{2(i-1)}, \tag{5}$$

where $I_0(\lambda)$ is the source spectrum and $R(\lambda)$ is the reflection spectrum of the FBG. The measurement error of the Bragg wavelength caused by the spectral distortion in a 1000 FBG network is less than 20 pm when the peak reflectivity of the identical FBGs is less than −35 dB [11]. For online writing ultra-weak FBGs, the stochastic wavelength fluctuation of the peak wavelength falls in a ± 50 pm range [12], and the spectral shadowing at the peak wavelength will be weaker when the reflectivity of FBG is less than −35 dB. Therefore, the error caused by spectral shadowing should be less than 20 pm. To verify spectral shadowing, the array that contains 1000 ultra-weak FBGs with peak reflectivity of −47 dB to −51 dB is prepared. The reflection spectra of the first FBG (in the forward direction), which is under strain and no strain, were detected from the two ends of the array (see Fig. 3). To avoid spectral shadowing, the first FBG is loaded by strain to shift its peak wavelength from the identical wavelength, which is 1551.172 nm at room temperature of 25 °C. Without strain, the difference of peak power measured from the two ends is 2.15 dB and the shift of the peak wavelength is less than 8 pm. The loss mainly induced by the transmission is 2.12 dB. Therefore, the insertion loss and the wavelength variation caused by the spectra shadowing can be neglected, and the maximum multiplexed number of TDM identical FBGs, with peak reflectivity of −47 dB to −51 dB, can be more than 1000. Given the zero spectral shadowing in the traditional WDM-FBG array, increasing the number of FBG sensors through multiplexing TDM sub-arrays at different wavelengths is feasible. Considering that a 4 nm light source at the center wavelength of 1551 nm has been configured, the TDM + WDM array can multiplex two TDM sub-arrays with a center wavelength of 1550 and 1552 nm. Each sub-array can contain 1000 identical FBGs.

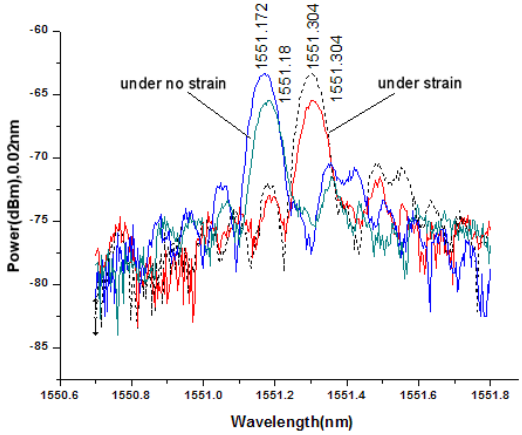

Fig. 3. Reflection spectra of the first FBG detected from the two ends of the FBG array.

A new crosstalk termed as *multiple-pulse crosstalk* will occur when the frequency of the pulse train is high enough. The multi-pulse crosstalk describes the spectral distortion of the upstream FBGs induced by the false signal of the previous pulses, which is reflected from the downstream FBGs and arrive at the detector at the same time with the real signal of upstream FBGs. The second pulse launches later than the first pulse for successive pulses. The interval between two pulses is T; thus, the time delay t_i is the round-trip time of the first pulse from

#194091 - $15.00 USD Received 17 Jul 2013; revised 12 Sep 2013; accepted 16 Sep 2013; published 20 Sep 2013

the *i*th FBG. To ensure a single pulse round-trip in the array, the relationship between T and t_i can be expressed as

$$T > t_i = c/[2n*(i-1)*d], \tag{6}$$

where T is the period of the pulse train. Multiple-pulse crosstalk can be avoided when T is larger than t_i. Therefore, when the period of the pulse train is required, the length of the TDM array without multiple-pulse crosstalk will be restrained. For example, the maximum length of the TDM array should be less than about 2 km because the period of the pulse train is 20 ms.

3.3 Interrogation Experiment

With the automated on-line writing system, two sub-arrays were fabricated in SMF-28 fiber and then spliced together. Every sub-array contained 1000 FBGs with center wavelengths of 1551.17 nm and 1552.05 nm. After 20 d of aging under the temperature of 80 °C, the peak reflectivity of the array was stable in the range of −47 dB to −51 dB. The separation distance between FBGs was 2 m. The bandwidth at −0.5 dB of the source was 2.92 nm. The modulation frequency was 40 kHz and the "on" time of SOA was 16 ns.

Single point and multi-point scanning measurement were performed to demonstrate the outstanding interrogation capability of the sensing network. The 1000th FBG was installed on the metal cantilever beam, and the strain resulting from the deflection of the free end was monitored by keeping the time delay of the 1000th FBG (see Fig. 4). The results show a measurement rate of 100 Hz for the 1000th FBG. Moreover, 2000 ultra-weak FBGs were interrogated in turns by employing the PC remote control, and the peak wavelengths of these FBGs were achieved (see Fig. 5). The interrogation speed based on the PC remote control was up to 100 FBGs per second. Considering that the control signal is transmitted via a general purpose interface bus, the interrogation time was mainly spent on the instruction generation of the operating system software and the conversion of data communication protocol. In the new design, the generator will be integrated into the CCD module to eliminate the operating system and low-speed communication. The interrogation speed is expected to be up to 5000 FBGs per second, which is limited by the maximum response speed of the CCD module.

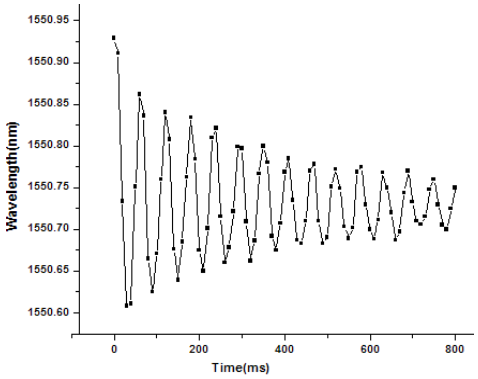

Fig. 4. Dynamic monitoring of the deflection of the free end.

#194091 - $15.00 USD Received 17 Jul 2013; revised 12 Sep 2013; accepted 16 Sep 2013; published 20 Sep 2013

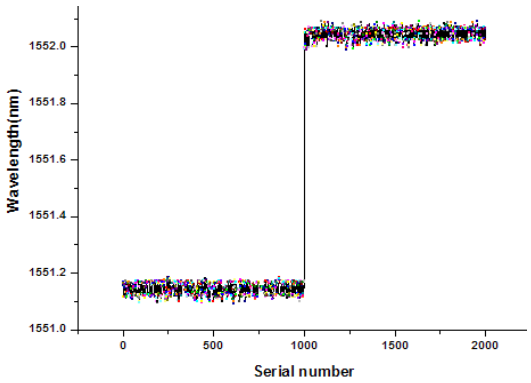

Fig. 5. The peak wavelengths of 2000 serial ultra-weak FBGs measured by PC remote control.

To investigate the OTDR performance of the sensing network, 10 FBGs of the array were interrogated by changing the time delay. The serial numbers for the FBGs were arranged as follows: 1 (under strain), 2, 3, 4, 5, 996, 997, 998, 999, and 1000. These numbers correspond to the following delays: 201, 221, 242, 263, 282, 20150, 20179, 20190, 20211, and 20230 ns. Figure 6 presents the reflected spectra of these FBGs. For the glass fiber used, 1 ns of time delay corresponds to the round distance of 0.1 m, and the theoretical difference of time delay between two adjacent FBGs is 20 ns, which is close to the measured value. An error of less than 2 ns is mainly induced by the non-ideal shape of the modulated pulse. For the first FBG, the round distance within 201 ns includes the pigtails of the optic jumper, the circulator, and EDFA. The total length of the pigtails is 8.5 m and the distance between SOA1 and the first FBG is 10.05 m. Therefore, the spatial position of the first FBG along the fiber is 1.55 m. On the basis of the time delay, the dead zone of the OTDR is only dependent on the pulse width, which is the round distance within a half of the pulse width. For example, a dead zone of 1 m is related to a pulse width of 20 ns.

Distributed temperature was measured to investigate the sensing performance of the network. Two sections of the sensor array, containing 20 FBGs, were heated in a high-low temperature test chamber (SIDA TEMI300), whereas the rest of the FBG sensors were kept at a room temperature of 25 °C [14, 15]. The chamber temperature was increased from 25 °C to 90 °C at a step of 5 °C and accuracy of 0.1 °C. At each step, the temperature was first kept for half an hour to ensure the accuracy of 0.1 °C and was then measured. Figure 7 shows the result of temperature measurement. The peak wavelengths of the heated FBGs shifted with increasing temperature. Figure 8 shows the relationship between the wavelength shift and the temperature. The measurement data of each FBG was fitted to obtain its temperature sensitivity, and the fitted coefficients are within the range of 10.2 pm/°C to 10.8 pm/°C. This finding is similar to the temperature characteristic of the ordinary grating. The variation is mainly caused by the measurement errors determined by the SNR of ultra-weak FBGs.

#194091 - $15.00 USD Received 17 Jul 2013; revised 12 Sep 2013; accepted 16 Sep 2013; published 20 Sep 2013

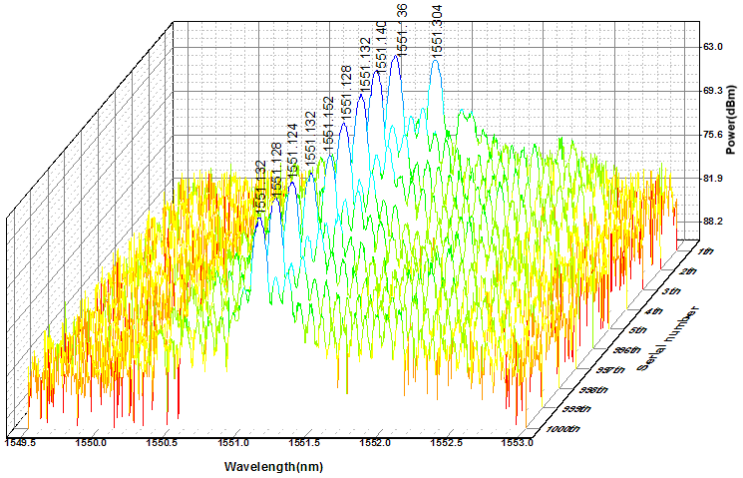

Fig. 6. Reflected spectra from 10 FBGs.

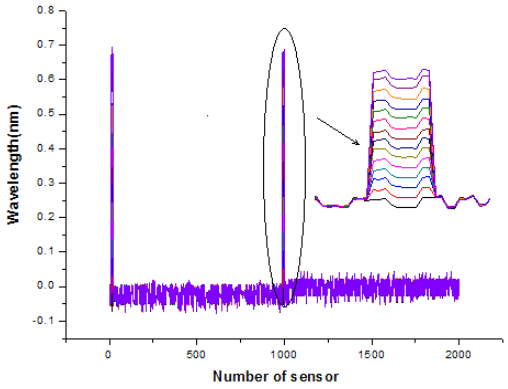

Fig. 7. Temperature measurement results of the 2000-sensor array.

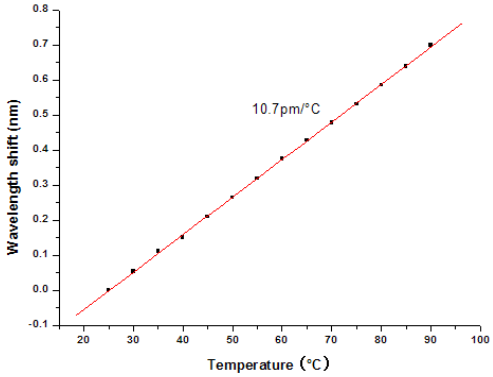

Fig. 8. Wavelength shift versus temperature change.

4. Conclusion

A novel large-scale ultra-weak FBG sensor network with two SOAs and one high-speed CCD module has been proposed and demonstrated. Results show that the proposed sensor network can interrogate the large-scale array at the speed of 100 FBGs per second and contain over

#194091 - $15.00 USD Received 17 Jul 2013; revised 12 Sep 2013; accepted 16 Sep 2013; published 20 Sep 2013

2000 FBGs by TDM + WDM. The pioneering design has low cost, weak crosstalk and good sensing characteristic. Therefore, the proposed design has a promising future for sensor application, in which large numbers of FBGs are needed.

Acknowledgments

This work was supported in part by the National Science Foundation of China, NSFC (Grant No. 61205070), and the Major Program of the National Natural Science Foundation of China, NSFC (Grant No. 61290311).

#194091 - $15.00 USD Received 17 Jul 2013; revised 12 Sep 2013; accepted 16 Sep 2013; published 20 Sep 2013